

# Static aerodynamic force coefficients for an arch bridge girder with two cross sections

Jian Guo\* and Minjun Zhu<sup>a</sup>

*Institute of Bridge Engineering, Zhejiang University of Technology, 288 Liuhe Road Hangzhou 310023, China*

*(Received April 29, 2019, Revised March 20, 2020, Accepted July 28, 2020)*

**Abstract.** Aiming at the wind-resistant design of a sea-crossing arch bridge, the static aerodynamic coefficients of its girder (composed of stretches of  $\pi$ -shaped cross-section and box cross-section) were studied by using computational fluid dynamics (CFD) numerical simulation and wind tunnel test. Based on the comparison between numerical simulation, wind tunnel test and specification recommendation, a combined calculation method for the horizontal force coefficient of intermediate and small span bridges is proposed. The results show that the two-dimensional CFD numerical simulations of the individual cross sections are sufficient to meet the accuracy requirements of engineering practice.

**Keywords:** static aerodynamic force coefficients; numerical simulation; girder; wind tunnel test; arch bridge

## 1. Introduction

The coastal areas of the East China are frequently subjected to typhoons and monsoons, where there was an average of 7.2 typhoons landing each year (Zhang *et al.* 2013). Typhoons are an important weather system that affect the bridge safety. Wind disasters have been taken as predominant as one of the top ten extreme weather events in the world. For example, the No. 16 of super-typhoon, the Rosa reached maximum wind speed of 33 m/s near the typhoon center when it landed China, causing economic losses of \$ 1.2 billion in Zhejiang. The instantaneous wind speed of the No. 23 typhoon Fete exceeded 61 m/s, causing economic losses of about \$ 1.5 billion and 6.314 million victims in Zhejiang Province. In recent years, the number and frequency of typhoons landed on the East China Sea have shown an increasing trend, which seriously threatens the safety of coastal infrastructure. Furthermore, with the increasing number of sea-crossing bridges in bay areas, the wind-resistant safety of bridges was the focus (Hu *et al.* 2013). For example, some sea-crossing bridges in Zhejiang Province have a basic wind speed of more than 40 m/s at the height of 10 meters.

In engineering design, there are several kinds of section types to be used, especially of  $\pi$ -shaped cross-section and streamline-shaped cross-section. At present, the main girder of lots of arch bridges and cable-stayed bridges have more than one cross-section. It is characterized by adopting a streamlined cross-section in the stayed cable or sling anchor area and a  $\pi$ -shaped cross-section in the cableless area. This girder form not only ensures the force transmission of the

sling anchorage area, but also reduces the material usage of the girder, which is a very competitive design scheme in economic advantages and mechanical properties. However, due to the different cross-sections along the bridge, the wind resistance and wind load are more complicated than the single section. The main girder of the arch bridge will cause different turbulence patterns when the wind flows through the arch bridge with different cross-sections, which will form different wind load effects on the girder. In high wind speed areas, it tends to become a control load for structural design. Therefore, it is crucial to determine the static aerodynamic coefficients of the main girder of arch bridges with various cross-sections. For the streamline-shaped section, the wind resistance to the bridge structure can be significantly reduced. In 1964, the Severn Bridge in the UK took the lead in the use of streamlined flat steel box girders. Since then, for large span and middle span bridges with the outstanding effect of wind resistance, the streamline-sections have predominantly advantage to be used.

Lu *et al.* (2005) used wind tunnel test and numerical simulation to select the cross-section of steel box girder of the Xihoumen Bridge with different slot width. Although the wind tunnel test is the most accurate method to study the bridge wind engineering (Wan *et al.* 2017), it has a high cost and a long period. At present, many researches (Wang *et al.* 2016, Qu and Liu 2007, Hallak *et al.* 2013, Guo *et al.* 2020) are based on numerical simulation. Selvam *et al.* (2010) took the East Bridge of the Danish Sea Belt as an example to calculate static aerodynamic force coefficients with two-dimensional and three-dimensional numerical simulations. The study shows that when the Reynolds number was bigger than 50000, the two-dimensional simulation is pretty much accurate, so it is proposed that in the wind-resistant design of bridges, two-dimensional simulation can be used to determine the static aerodynamic force coefficients for structural wind resistance calculation. Rocchi *et al.* (2015) conducted the static aerodynamic force

\*Corresponding author, Professor

E-mail: [guoj@zjut.edu.cn](mailto:guoj@zjut.edu.cn)

<sup>a</sup>Master

E-mail: [zmj@zjut.edu.cn](mailto:zmj@zjut.edu.cn)

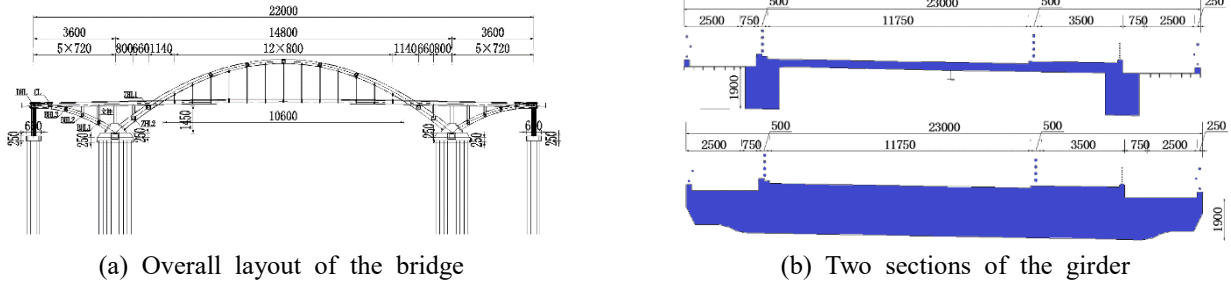


Fig. 1 Dimension of bridge structure

coefficients by studying on a streamlined box girder by

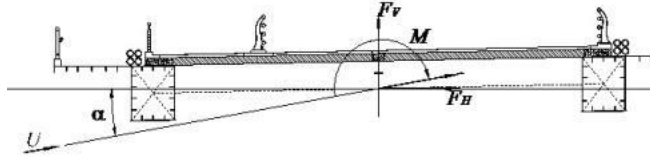


Fig. 2 Static aerodynamic coordinate system of girder section

means of experimental and two-dimensional CFD numerical simulation. The study shows that it is feasible to determine the static aerodynamic force coefficients of the main girder by two-dimensional CFD numerical simulation, the CFD numerical simulation may help in minimizing the discretization error in the design stage of the wind tunnel tests. In the past, the wind resistance of streamline cross-section is generally considered to be greater than that of  $\pi$ -shaped cross-section. However, Chen (2017) proposed: When the wind-induced vibration of the bridge is in large displacement vibration, the structure will still be in a safe state, which is different from the existing theory of critical wind speed in wind-induced vibration analysis. However, the  $\pi$ -shaped cross-section may have a higher critical wind speed than the streamlined cross-section. This is a significant research direction for bridge wind engineering in the future. Some bridges that use  $\pi$ -shaped cross-section girders have also been analyzed under the wind loads.

The girder bridge analyzed in this paper is composed of stretches of  $\pi$ -shaped and box sections alternating along the span length. The static aerodynamic coefficients of these cross-sections were calculated by means of 2D CFD numerical simulations and those of the sea crossing arch bridge girder through wind tunnel test. By comparing the wind resistance performance of the two individual cross-sections and that of the bridge girder, this paper proposes the use of a simplified method to calculate the static aerodynamic coefficients of the complex girder, in order to serve the engineering design.

## 2. Static aerodynamic force coefficients of arch bridge girder

### 2.1 Engineering background

The overall layout of a sea-crossing arch bridge in Zhejiang and the cross-sections of the main girder are

shown in Fig. 1. 85% of the main girder cross-section is the  $\pi$ -shaped cross-section, 15% is the box cross-section. The bridge is a three-span continuous arch bridge with spans of 36 + 148 + 36 m. The arch rib height is 37 m/s and the rise-span ratio is 1/4. The bridge is in high wind speed areas, and the basic wind speed is 40.5 m/s at 10m height.

### 2.2 static aerodynamic force coefficients of girder

As shown in Fig. 2, the static aerodynamic force which acts on the girder can be expressed by the vertical force  $F_V$ , the horizontal force  $F_H$  and the longitudinal axis aerodynamic pitching torque  $M$ ,  $\alpha$  is the wind attack angle which is positive when the mean wind direction is upward.

The static aerodynamic force coefficients under the body axis system are defined as follows (Chen 2005, Mao *et al.* 2017):

$$\text{Horizontal force coefficient: } C_H = \frac{F_H}{1/2\rho U^2 H} \quad (1)$$

$$\text{Vertical force coefficient: } C_V = \frac{F_V}{1/2\rho U^2 B} \quad (2)$$

$$\text{Torque coefficient: } C_M = \frac{M}{1/2\rho U^2 B^2} \quad (3)$$

Where  $U$  is the wind speed;  $\rho$  is air density;  $F_H$ ,  $F_V$ , and  $M$  are the horizontal force, vertical force, and torque, respectively;  $B$  and  $H$  are the width and height of the girder cross-section, respectively.

### 2.3 Bridge specification calculation method of horizontal force coefficient

The wind-resistant design specification for highway bridges in China (JTG / T D60-01-2004) stipulates that the simplified equation can be used to calculate the horizontal force coefficient for Bridges with a span of less than 200 m. Where the horizontal force coefficient  $C_H$  of I-girder,  $\pi$ -girder and box-girder can be calculated as follows

$$C_H = \begin{cases} 2.1 - 0.1\left(\frac{B}{H}\right) & 1 \leq \frac{B}{H} \leq 8 \\ 1.3 & 8 \leq \frac{B}{H} \end{cases} \quad (4)$$

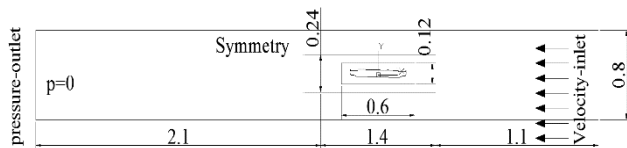


Fig. 3 Calculation area

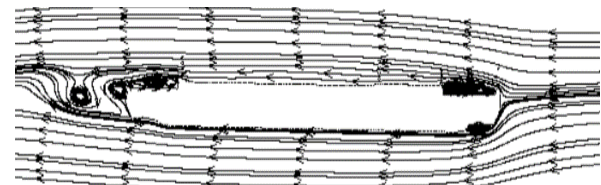
Where  $B$  is the width of the girder (m),  $H$  is the projection height of the girder (m) which considering the height of ancillary facilities.

It can be seen from Eq. (4) that the calculation method of the horizontal force coefficient in the specification is based on the aspect ratio of the cross-section. However, it does not consider the variation of the horizontal force coefficient when the wind attack angle is different from  $-7^\circ$  to  $7^\circ$ . This is allowable for the design of a middle and small span bridge. However, for bridge design in high wind speed areas, in order to optimize selections for different cross-sections, especially for the main girder with different cross-sections, more detailed consideration should be given to the wind resistance performance of the bridge.

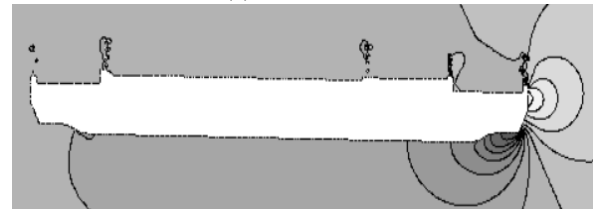
### 3. Numerical simulation

From the existing research (Zhang *et al.* 2016, Tan and Chen 2009, Li *et al.* 2013, Liu *et al.* 2010, Li *et al.* 2017, Menter 1994), the three-dimensional simulation of CFD needs to consume much time and storage, and when the structure is complex, the accurate simulation of detail component is difficult. However, the two-dimensional simulation method is accurate enough to obtain the static aerodynamic force coefficients of bridges. The CFD simulation was carried out by FLUENT in this paper, and the CFD model is constructed with a scale ratio of 1:50. The wind attack angle varies from  $+7^\circ$  to  $-7^\circ$ , every  $1^\circ$  is a test condition and the wind speed is 10 m/s. The box cross-section and the  $\pi$ -shaped cross-section are modeled separately. In some research works (Zhang *et al.* 2016), numerical simulation usually ignored ancillary facilities such as guardrails, but the author finds that the obstacles such as ancillary facilities can also interfere with the wind field, it makes the wind field around the bridge more complex (Kim *et al.* 2011, Kwon *et al.* 2011). Therefore, guardrails are considered in the numerical simulation. For the two-dimensional flow field, the distance from the boundary to the model should be 20 times larger than the model size (Tan and Chen 2009), and the calculation area set by taking section (b) as an example is shown in Fig. 3.

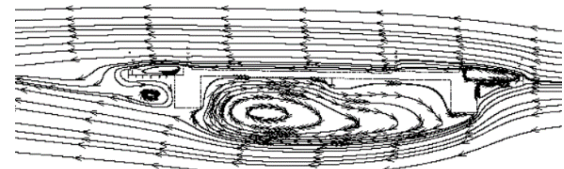
The calculation area is a rectangle of  $4.6\text{ m} \times 0.8\text{ m}$ , and the calculation area is modeled using a structured mesh. The refined mesh is used around the girder where the flow field changes drastically, and the area where the flow field changes gently uses sparse mesh. The reasonable meshed are adopted in the flow field transition region. The number of elements in mesh of each model is between 370000 and 410000. The right boundary is the velocity-inlet, the left boundary is the pressure-outlet, and the pressure is zero. The upper and lower boundaries are symmetry (Xu 2013).



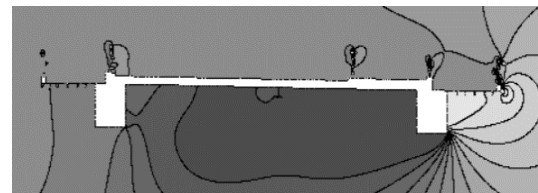
(a) Streamline



(b) Pressure field

 Fig. 4 Distribution of the streamline and pressure field of the box cross-section under  $0^\circ$ 


(a) streamline



(b) Pressure field

 Fig. 5 Distribution of the streamline and pressure field of the  $\pi$ -shaped cross-section under  $0^\circ$ 

For the numerical simulation of the static aerodynamic force coefficients of the streamlined bridge section,  $k-\epsilon$  Model should be adopted which the calculation results can meet the accuracy requirements (Li *et al.* 2013, Liu *et al.* 2010). The two-equation turbulence model has a turbulence intensity of 0.5 and a turbulent viscosity ratio of 10. The pressure-velocity coupled is solved using the SIMPLEC method. The pressure equation is discretized in a second-order scheme. The momentum equation, the turbulent kinetic energy equation and the turbulent dissipation rate equation both adopt a second-order upwind differential scheme. The streamline and the pressure field near  $0^\circ$  wind attack angle are shown in Figs .4 and 5, respectively.

The results of the numerical simulation are shown in Fig. 6, the wind resistance performance of the two cross-sections was much different, especially for the horizontal force coefficient, the difference between them is 60% to 90%. For the vertical force coefficient, the calculation results of the two cross-sections were close. For the torque coefficient, there are some errors in the small attack angle. From the above results, it is not advisable to use the numerical simulation results of one cross-section to replace the static aerodynamic coefficients of the whole girder.

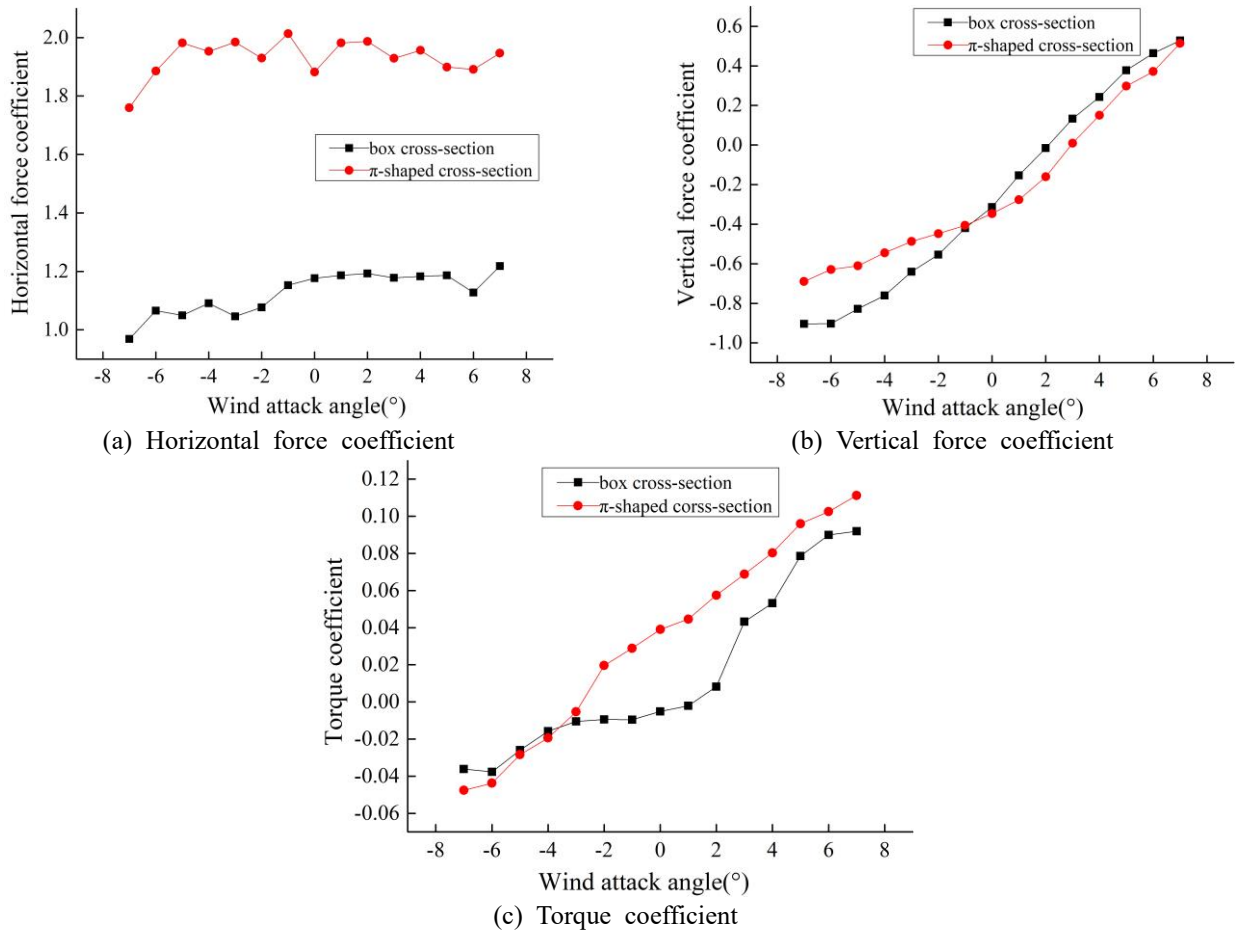


Fig. 6 Comparison between static aerodynamic force coefficients of two sections

Nevertheless, considering the proportion of the  $\pi$ -shaped cross-section in the total bridge cross-section, the  $\pi$ -shaped cross-section may be closer to the actual bridge. In order to verify the results of the numerical simulation, further wind tunnel tests were carried out.

#### 4. Wind tunnel test

In order to analyze the wind resistance characteristics of the girder of the sea-crossing arch bridge more accurately, the section model wind tunnel test of the girders was carried out. The scale ratio of section model and numerical simulation is the same as 1:50. As shown in Figs. 7 and 8, the length of the bridge model is 0.96 m, the width is 0.46 m, and the height is 0.038 m (The height excluding the ancillary facilities).

The test was carried out in a boundary layer wind tunnel, which is a closed vertical flow low speed wind tunnel with an air density of  $1.18 \text{ kg/m}^3$ , the test section length is 18 meters, the width is 4 m and the height is 3 m. The wind speed range is continuously adjustable from 3-55 m/s, the performance of the wind tunnel flow field is extremely good. The cross-sectional speed non-uniformity of the vacant wind tunnel is less than 1.0% at 40 m/s, the turbulence intensity is less than 0.5%, and the average airflow declination is less than  $0.5^\circ$ . The section model is

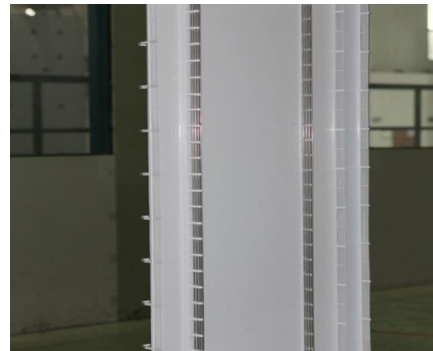


Fig. 7 The positive view of section model



Fig. 8 The back view of section model

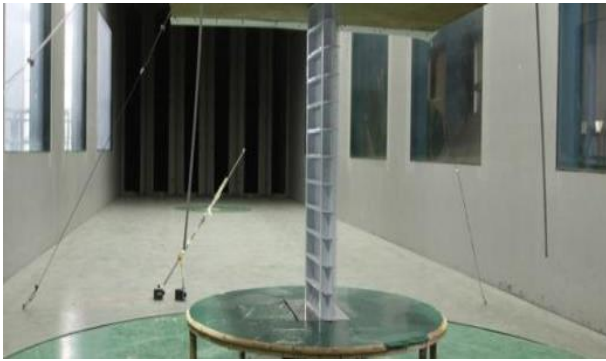


Fig. 9 Wind tunnel test with section model

installed vertically on the turntable. As shown in Fig. 9, in order to eliminate the influence of the bottom boundary layer and the top airflow over the section model (producing an ideal two-dimensional flow field for the section model), the model is raised and endplates are set on both sides during the test. The test was carried out at two wind speeds, 10 m/s and 14.5 m/s, respectively. The wind attack angle is  $-7^{\circ}\sim 7^{\circ}$ , and each  $1^{\circ}$  is a test condition. The sampling time of each working condition is 1 minute, and the sampling frequency is 300 Hz. The static aerodynamic coefficients measured under the two wind speeds were very close. This paper only studied the test condition of 10 m/s.

### 5. Comparison of calculation and wind tunnel test results

Based on numerical simulation, wind tunnel tests and specification recommendations, the curve of the static aerodynamic force coefficients of the  $\pi$ -shaped cross-section and box cross-section under the wind attack angle ( $-7^{\circ}\sim 7^{\circ}$ ) was plotted. As shown in the Figs. 10, 11 and 12, the results of numerical simulation are compared with the wind tunnel test. For the horizontal force coefficient, the simulation results of the  $\pi$ -shaped cross-section were closer to the wind tunnel test than the box cross-section, but the  $\pi$ -shaped cross-section simulation results were generally larger than the wind tunnel test results, and the box cross-section was generally smaller than the wind tunnel test. This is mainly because the actual bridge is a combination of two cross-sections. In terms of the vertical force coefficient and the torque coefficient, the simulation results of the  $\pi$ -shaped cross-section were closer to the wind tunnel test results than the box cross-section. However, with the increase of the wind attack angle, the difference in the vertical force coefficient and torque coefficient between the numerical simulation and the wind tunnel test was also increasing. One reason is that the separation and reattachment of airflow, the shedding and generation of vortices result in the complicated flow field, which affects the accuracy of the numerical calculation in the large wind attack angle. Another reason is that the mesh division in the ancillary facilities is complex. Due to the limitation of computer performance, the mesh quality in the auxiliary facilities is slightly reduced on the premise of ensuring the calculation accuracy.

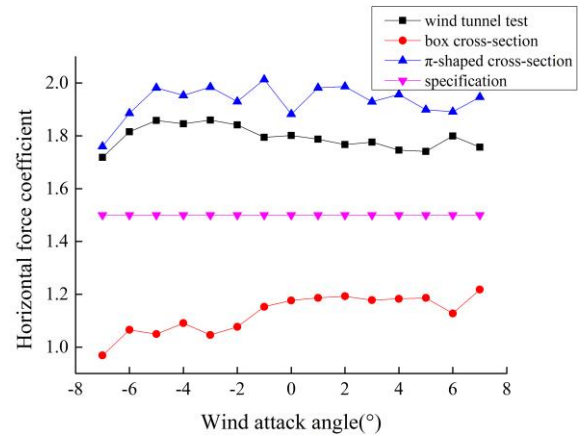


Fig. 10 Comparisons of horizontal force coefficient

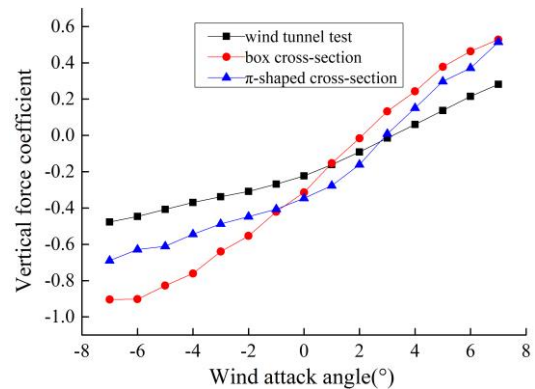


Fig. 11 Comparisons of vertical force coefficient

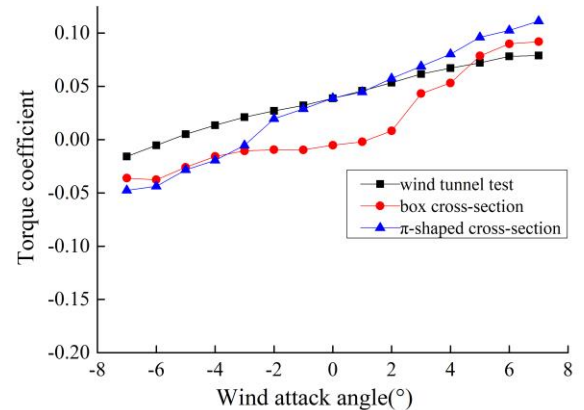


Fig. 12 Comparisons of torque coefficient

### 6. Combined calculation method

Because  $\pi$ -shaped accounts for 85% of the cross-section, the contribution of  $\pi$ -shaped cross-section to the horizontal force coefficient was dominant. The simulation results of  $\pi$ -shaped cross-section were closer to the actual bridge than that of box cross-section, and the horizontal force coefficient of wind tunnel test was more than 15% larger than that calculated by the specification. In engineering applications, a simple and accurate calculation method is often needed to determine the horizontal force coefficient of the middle and small span bridges. For the girder of the arch bridge with different cross-sections, the horizontal

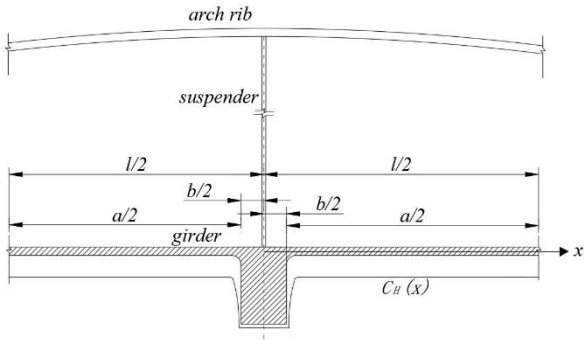


Fig. 13 Drag coefficient calculation

force coefficient is variable along the direction of girder, as shown in Fig. 13. the horizontal force coefficient of girder is the horizontal force per unit length, as shown in Eq. (5).

$$\overline{C_H} = \frac{\int_{-l/2}^{l/2} C_H(x) dx}{l} \quad (5)$$

Where  $x$  is the length of abscissa (m),  $l$  is the length of girder (m),  $C_H(x)$  is the horizontal force coefficient of cross-section  $x$ .

Considering the girder is composed of two sections, Eq. (5) can be simplified to Eq. (6)

$$\begin{aligned} \overline{C_H} &= \frac{\int_{-l/2}^{-b/2} C_H^1(x) dx + \int_{-b/2}^{-a/2} C_H^2(x) dx + \int_{-a/2}^{l/2} C_H^1(x) dx}{l} \\ &= \frac{2 \int_{-b/2}^{-a/2} C_H^1(x) dx + \int_{-b/2}^{-a/2} C_H^2(x) dx}{l} \\ &= \frac{a}{l} \overline{C_H^1} + \frac{B}{l} \overline{C_H^2} \end{aligned} \quad (6)$$

Where  $\overline{C_H^1}$  is the mean horizontal force coefficient of the  $\pi$ -shaped cross-section from pressure integration along the portion of the bridge,  $\overline{C_H^2}$  is the mean horizontal force coefficient of the box cross-section from pressure integration along the portion of the bridge. In the neighborhood of the section discontinuity, the presence of an abrupt change of section disturbs the flow, therefore,  $\overline{C_H^1}$  and  $\overline{C_H^2}$  are approximate to mean horizontal force coefficient of the two cross-sections obtained from 2D analyses.  $a$  is the length of the girder with  $\pi$ -shaped cross-section,  $b$  is the length of the girder with box-section.

In this paper,  $a/l$  is 0.85 and  $b/l$  is 0.15. Taking the wind tunnel test results as the standard value, the error of between the numerical simulation and combined calculation (Eq. (6)) and the wind tunnel test were plotted, which is shown in Fig. 14. From Fig. 14, it can be found that the horizontal force coefficient calculated by Eq. (6) is closer to the wind tunnel test value, and the error between them is within  $\pm 5\%$ . The error of the  $\pi$ -shaped cross-section and the wind tunnel test generally reached more than 5%; the error

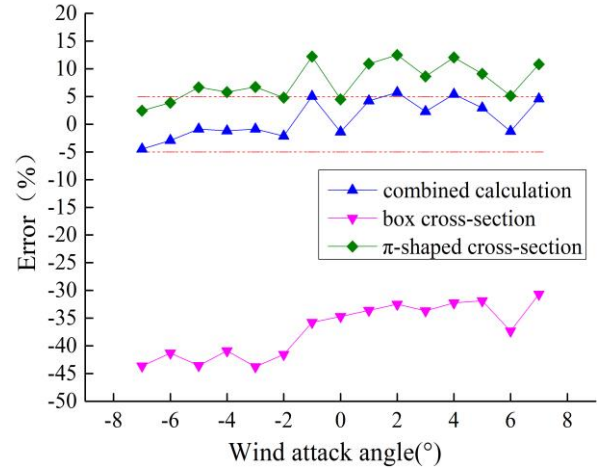


Fig. 14 Comparison between numerical simulation and wind tunnel test

Table 1 Comparisons of horizontal wind load of three methods with wind tunnel test

Wind attack angle (°)	Error between numerical simulation and wind tunnel test	Error between combined calculation and wind tunnel test	Error between Specification calculation and wind tunnel test	Error between Specification calculation* and wind tunnel test
	(%)	(%)	(%)	(%)
7	10.82	4.59	53.51	-14.62
6	5.10	-1.27	50.05	-16.64
5	9.08	2.94	55.24	-13.84
4	12.05	5.41	54.92	-14.08
3	8.62	2.28	52.40	-15.53
2	12.47	5.72	53.25	-15.10
1	10.09	4.23	51.53	-16.06
0	4.48	-1.39	50.33	-16.74
-1	12.21	5.01	50.90	-16.41
-2	4.78	-2.16	47.03	-18.54
-3	6.70	-0.87	45.51	-19.35
-4	5.80	-1.20	46.55	-18.73
-5	6.65	-0.88	45.45	-19.27
-6	3.87	-2.91	48.76	-17.36
-7	2.42	-4.49	56.94	-12.71

\*: Height of ancillary facilities are not considered

of box cross-section generally reached -30%. Although there are some errors in the calculation of the combined method due to the abrupt change of section disturbs the flow in the neighborhood of the section discontinuity, but from the calculation results, the influence is relatively slight, and the combined calculation method still conforms to the engineering error.

For design, the horizontal wind loads directly determine the selection and construction of the girder cross-section, therefore it is very important to get wind load accurately. According to Eq. (1), the horizontal wind loads on arch bridges can be directly calculated by using horizontal force coefficients. When calculating the wind load according to

the specification, the projected height of the girder includes the height of the ancillary facilities.

Here, according to the numerical simulation, wind tunnel test, bridge specification and combined calculation method, the horizontal wind loads were calculated at the respective attack angles at 10 m/s wind speed, and the horizontal wind load obtained by the wind tunnel test was used as the standard value. Comparing the results of CFD simulation, combined calculation, specification calculation with wind tunnel test, the error of horizontal wind loads was shown in Table 1.

It clearly showed that among the three methods, the horizontal wind load calculated by the combination calculation method (Eq. (7) at each wind attack angle was the closest to the test value. The horizontal wind loads calculated by the  $\pi$ -shaped cross-section simulation was slightly larger than the test value at each angle. In addition, the horizontal wind loads calculated by the specification without considering the height of ancillary facilities was lower than the test value by about 15%. The horizontal wind loads calculated by the specification with considering the height of ancillary facilities was higher than the test value by about 50%, it is safe for middle and small span bridges whose wind loads is not the control load. But for girders in high wind speed areas, the specification calculation will overestimate the horizontal wind loads. In order to obtain more accurate horizontal wind load values, the numerical simulation can be carried out for different sections, and then the combination calculation can be carried out. The results obtained have better accuracy.

## 6. Conclusions

In this paper, the wind tunnel test of the section model of the sea-crossing arch bridge was completed. The numerical calculation of the two different girder sections was carried out by CFD, and the static aerodynamic force coefficients were obtained. Considering the complexity of the girder, the static aerodynamic force coefficients calculated by numerical simulation, wind tunnel test and specification are compared. A combined calculation method of horizontal force coefficient was proposed to apply to the multi cross-section girder. Based on the wind load of girders that need to be considered in engineering design, three calculation methods were compared and analyzed. The following conclusions are as follows:

- The static aerodynamic coefficients are mainly affected by the shape of the cross-section. There is an obvious difference in the aerodynamic coefficients of  $\pi$ -shaped cross-section and box cross-section, especially in the horizontal force coefficient, the difference between the two is more than 52%, while the difference between the vertical force coefficient and the torque moment coefficient is not significant.
- The application of 2D numerical simulation can make a more accurate analysis of a single cross-section, and the simplified calculation based on the combined calculation method is conducive to the rapid and accurate calculation of the horizontal force coefficient of

the multi-section girder in the engineering design.

- The combined calculation method was tested for a girder composed of stretches of two cross sections with the same height in this paper, but the application of this method in cases of girder with sections of different heights is expected to produce greater errors due to flow disturbance in the section discontinuities. This method is mainly used in the wind-resistant design and section selection of middle and small span bridges.
- The simplified calculation method of the horizontal force coefficient in the bridge specification (China) is more suitable for the girder with a kind of section. The calculation of the specification is a simplified method, which does not consider the effect of the variation of wind attack angle on the static aerodynamic force coefficients. However, the calculated values of the bridge specifications have a safety factor of about 1.5 times for the horizontal wind loads, and the design of wind resistance is safe enough.

## Acknowledgments

The research described in this paper was financially supported by the National Key R&D Program of China (2018YFC0809604, 2016YFC0802201) and the National Natural Science Foundation of China (U1709207, 51578506).

## References

- Chen, Z.Q. (2005), *Bridge Wind Engineering*, China Communications Press, Beijing, China.
- Chen, Z.Q. (2017), "Design theory calls for source innovation: thinking of "cast-in-situ" and "critical wind speed", *The 7th Forum of Bridge and Tunnel Engineering Technology*, Hangzhou, China, September.
- Guo, J., Zhu, M.J. and Hu, C.J. (2020), "Study on wind load shape factor of long-span stadium roof", *J. Adva. Struct. Eng.*, <https://doi.org/10.1177/1369433220908111>.
- Hallak, P.H., Pfeil, M.S., de Oliveira, S.R., Battista, R.C., de Sampaio, P.A. and Bezerra, C.M. (2013), "Aerodynamic behavior analysis of Rio-Niterói bridge by means of computational fluid dynamics" *J. Eng. Struct.*, **56**(56), 935-944. <https://doi.org/10.1016/j.engstruct.2013.06.010>.
- Hu, L., Xu, Y.L. and Huang, W.F. (2013), "Typhoon-induced non-stationary buffeting response of long-span bridges in complex terrain", *J. Eng. Struct.*, **57**(4), 406-415. <https://doi.org/10.1016/j.engstruct.2013.09.044>.
- JTG/T D60-01-2004 (2004), *Wind-resistant Design Specification for Highway Bridges*, China Communications Press, Beijing, China.
- Kim, D.H., Kwon, S.D., Lee, I.K. and Jo, B.W. (2011), "Design criteria of wind barriers for traffic. Part 2: Decision making process", *J. Wind Struct.*, **14**(1), 55-70. <https://doi.org/10.12989/was.2011.14.1.071>.
- Kwon, S.D., Kim, D.H., Lee, S.H. and Song, H.S. (2011), "Design criteria of wind barriers for traffic. Part 1: Wind barrier performance", *J. Wind Struct.*, **14**(1), 55-70.
- Liu, Y., Chen, Z.Q. and Zhang, Z.T. (2010), "CFD numerical simulation for aerostatic coefficients of a box girder section", *J. Vib. Shock*, **29**(1), 133-137
- LU, G.C., ZHANG, H.F., YANG, Y.X. and GE, Y.J. (205), "Cross

- section aerodynamic optimization of steel box girder in Xihoumen Suspension Bridge preliminary design”, *J. Southwest Jiaotong Univ.*, **40**(4), 473-477.
- Mao, W.H. and Zhou, Z.Y. (2017), “Ground effects on wind-induced responses of a closed box girder”, *J. Wind Struct.*, **25**(4), 397-413. <https://doi.org/10.12989/was.2017.25.4.397>.
- Menter, F.R. (1994), “Two-equation eddy-viscosity Turbulence models for engineering applications”, *J. AIAA J.*, **32**(8), 269-289.
- Qu, W.L. and Liu, L.N. (2007), “CFD-based numerical research in the identifying of tri-component force coefficient of bridge”, *J. Wuhan Univ. Technol.*, **172**(7), 85-88.
- Rocchi, D., Argentini, T. and Sbroisi, M. (2015), “Pressure distribution and global forces on a bridge deck section: experimental and CFD analysis of static aerodynamic forces”, *J. Bridge Eng.*, **20**(9), 04014097. [https://doi.org/10.1061/\(ASCE\)BE.1943-5592.0000695](https://doi.org/10.1061/(ASCE)BE.1943-5592.0000695).
- Selvam, R.P., Bosch, H. and Joshi, R. (2010), “Comparison of 2D and 3D CFD modeling of bridge aerodynamics”, *The 5th International Symposium on Computational Wind Engineering (CWE2010)*, Chapel Hill, U.S.A, May.
- Su, Y., Xiang, H., Fang, C., Wang, L. and Li, Y. (2017), “Wind tunnel tests on flow fields of full-scale railway wind barriers” *J. Wind Struct.*, **24**(2), 171-184. <https://doi.org/10.12989/was.2017.24.2.171>.
- Tan, H.X. and Chen, Z.Q. (2009), “Application of CFD in calculating static coefficients of bridge section”, *J. Eng. Mech.*, **26**(11), 68-72.
- Wan, J.W., Wang, Q., Liao, H.L. and Li, M.S. (2017), “Study on aerodynamic coefficients and responses of the integrated catwalk of Halogaland Bridge”, *J. Wind Struct.*, **25**(3), 215-232. <https://doi.org/10.12989/was.2017.25.3.215>.
- Wang, J.J., Fan, J.S. and Yang, X.G. (2016), “Computational study on Static coefficient of box girder section for long-span bridges”, *Eng. Mech.*, **33**(1), 95-104.
- Weisheng, L.Y.A. and Haili, L.C.L. (2013), “Aerodynamic optimization of three-box-girder deck by CFD model” *J. China Civil Eng. J.*, **46**(1), 61-68.
- Xu, Y.L. (2013), *Wind Effects on Cable-supported Bridges*, John Wiley & Sons, Singapore.
- Zhang, Y.C., Fan, J.P. and Deng, H. (2013), “Forecasting of typhoon disaster loss in Zhejiang Province based on the combination forecasting model”, *J. Nat. Disasters*, **22**(6), 223-231.
- Zhang, Z.T., Zhang X.X. and Chen, Z.Q. (2016), “Status of the application of turbulence models in CFD simulations of bridge aerodynamic loads”, *Eng. Mech.*, **33**(6), 1-8.